Inorganic Chemistry Communications 36 (2013) 170–173

Contents lists available at ScienceDirect

Inorganic Chemistry Communications

journal homepage: www.elsevier.com/locate/inoche

Structure and physical properties of a hydrogen-bonded framework based on carboxyl-substituted TTF ligand and $Mn(ClO_4)_2$

Jie Qin [a,b,*], Long Cui [b]

[a] School of Life Science, Shandong University of Technology, Zibo 255049, PR China
[b] State Key Laboratory of Coordination Chemistry, School of Chemistry and Chemical Engineering, Nanjing University, Nanjing 210093, PR China

ARTICLE INFO

Article history:
Received 22 July 2013
Accepted 29 August 2013
Available online 4 September 2013

Keywords:
Tetrathiafulvalene
Carboxylic ligand
Hydron-bonding
Redox chemistry

ABSTRACT

The well-soluble tetrathiafulvalene carboxylic derivative $[Bu_4N]_2[TTF(COOH)_2(COO)_2]$ (**L**) has been used to create the interesting 3D supramolecular network $[Mn(H_2O)_4(CH_3OH)_2][TTF(COOH)_2(COO)_2]$ (**1**), driven by O–H···O interaction. The absorption spectra and electrochemical behavior of **L** and **1** have been discussed. Optimized conformation and molecular orbital diagram of **L** have been calculated with density functional theory.

The last decades witness tremendous progress of tetrathiafulvalene (TTF) derivatives in the field of material chemistry [1–3], owing to their unique π electron delocalized structure and attractive reversible redox property. In order to prepare bifunctional TTF derivatives, various mono- or polydentate coordinating functional groups have been attached to the TTF moiety. Among these functional groups, most attention has been focused on the N-heterocyclic based ligands, such as pyridine [4–7], 2,2′-bipyridine [8–10], and 1,10-phenanthroline [11,12].

Carboxylic derivatives are useful building blocks for the construction of metal–organic frameworks, due to their strong coordination ability and diverse coordination modes [13,14]. By carefully choosing appropriate carboxylic ligands and auxiliary ligands, we can obtain desirable architectures of MOFs [15–18] and carboxylate-polymers. Meanwhile, they are endowed with hydrogen-bonding capabilities to prepare intriguing supramolecular systems [19,20]. Whereas, little attention has been paid to TTF-carboxylic derivatives compared to the N-heterocyclic analogues [21,22].

In this paper, the tetrathiafulvalene carboxylic derivative $[Bu_4N]_2[TTF(COOH)_2(COO)_2]$ (**L**) which is well-soluble in common polar organic solvents has been successfully synthesized. Further reaction of **L** with $Mn(ClO_4)_2$•$6H_2O$ affords an interesting 3D supramolecular network $[Mn(H_2O)_4(CH_3OH)_2][TTF(COOH)_2(COO)_2]$ (**1**) (Scheme 1). The crystal structure, spectroscopic and electrochemical properties of **L** and **1** are investigated. Optimized conformation and molecular orbital diagram of **L** have been calculated with density functional theory.

As shown in Scheme 1, the precursor compound **II** was obtained by homocoupling of **I** in the presence of triethyl phosphite. Carboxylic ligand **L** was synthesized by alkaline hydrolysis and partial acidification of the ester groups of **II**, with high yields. **L** features remarkable good solubility in common polar organic solvents such as CH_2Cl_2, $CHCl_3$, CH_3CN, THF, etc, which potentially facilitates the further reaction with transition metal ions. Further reaction of **L** with $Mn(ClO_4)_2$•$6H_2O$ affords compound **1**. In IR spectra, the typical stretching band $\nu(C = O)$ of methoxycarbonyl groups for **II** occurs at 1745 cm^{-1}. While the strong symmetric stretching mode $\nu_{as}(COO^-)$ for **L** and **1** is clearly visible around 1421 cm^{-1}, and the asymmetric stretching mode $\nu_s(COO^-)$ is located at 1601 cm^{-1} and 1540 cm^{-1}, respectively.

The molecular structure of the anion of **L** is shown in Fig. S1 [23], the two carboxyl groups are deprotonated sharing the proton with the unprotonated ones to form a seven membered ring. It is worth noting that the anionic unit $[TTF(COOH)_2(COO)_2]^{2-}$ adopts the completely planar conformation, with a root-mean-square deviation of 0.000 Å from a least-squares plane through all the atoms. Single crystal analysis reveals, as shown in Fig. 1, complex **1** consists of the same anionic moiety as **L** and a $[Mn(H_2O)_4(CH_3OH)_2]$ cation [23]. The Mn(II) center adopts a quasi-octahedral coordination sphere consisting of water molecules in the equatorial plane, the average Mn1–O(H_2O) bond length is 2.133 Å. The methanol molecules occupy the axial positions with longer bond length of 2.259(2) Å for Mn1–O7. For the structure of anionic unit, the TTF unit is slightly twisted, the average deviation from a least-squares plane through all the atoms is 0.0231 Å. The deprotonated carboxyl group is twist −3.023(4)° from the TTF core, whereas the unprotonated carboxyl group is twisted 0.562(8)°.

In the solid state, for compound **L**, the anionic and cationic layers are arranged alternatively, no significant intermolecular interactions are

---

[*] Corresponding author at: School of Life Science, Shandong University of Technology, Zibo 255049, PR China. Tel.: +86 533 2780271.
E-mail address: qinjietutu@163.com (J. Qin).

1387-7003/$ – see front matter © 2013 Elsevier B.V. All rights reserved.
http://dx.doi.org/10.1016/j.inoche.2013.08.034

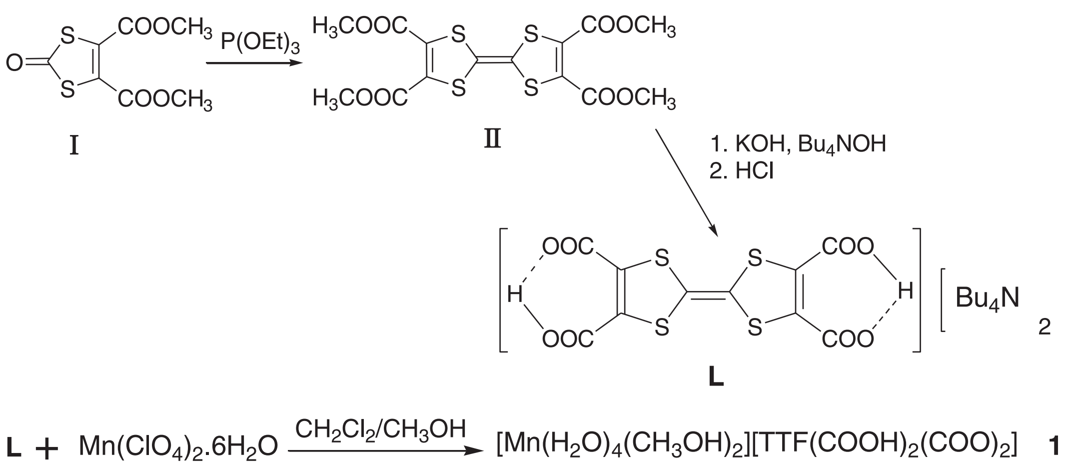

Scheme 1. Synthetic routes to compound **1**.

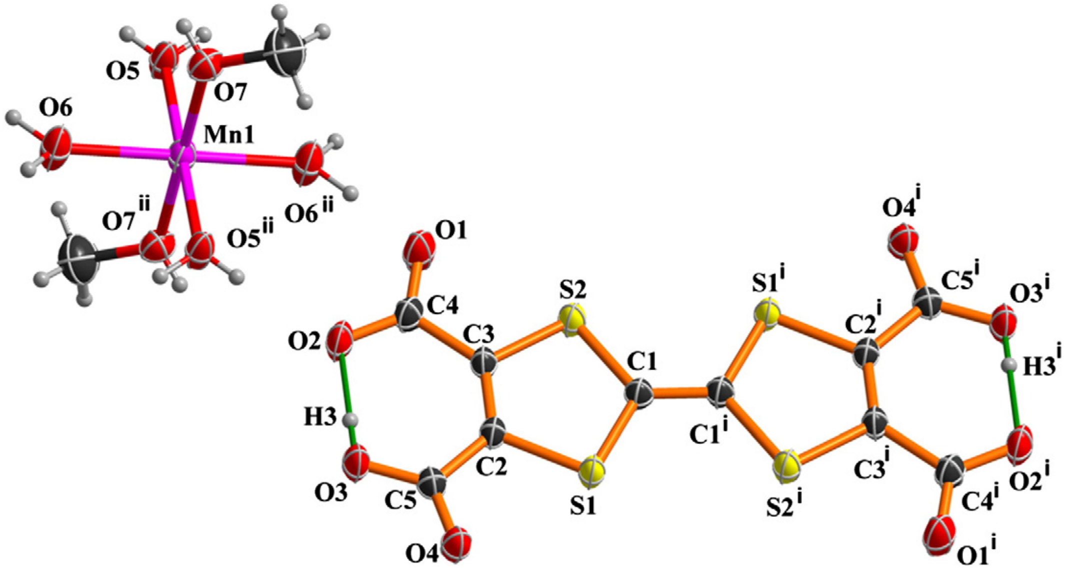

Fig. 1. ORTEP views of **1** with the atom-numbering scheme (50% probability displacement ellipsoids, symmetry codes: (i) –x − 1, –y + 2, –z; (ii) –x + 1, –y + 1, –z + 1).

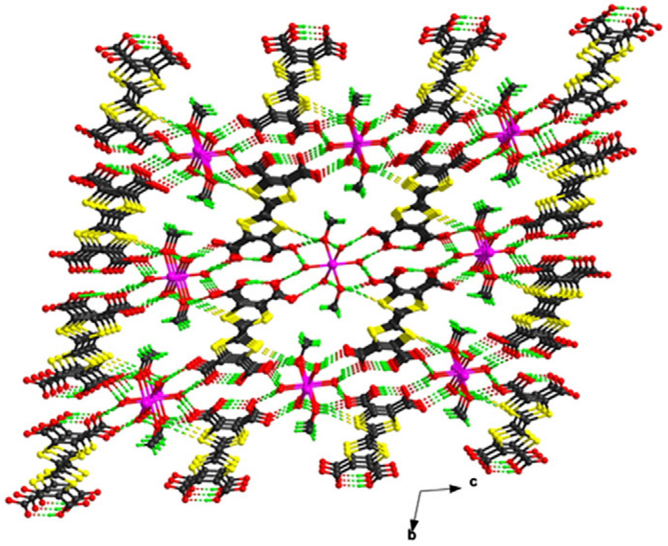

Fig. 2. A perspective view along the a axis of the three-dimensional hydrogen-bonded network in **1** (hydrogen-bonding interactions are shown as dashed lines).

found (Fig. S2). While in compound **1**, rich intermolecular hydrogen bonding interactions are observed. First of all, the inorganic Mn^{II} units are seized together through O(6)–H(6A)···O(7)$^{\#2}$, (symmetry code: #2 x + 1, y, z) to form 1D chainlike structure extended along the crystallographic a axis (Fig. S3). The Mn^{II}-chain is surrounded by organic $\{TTF(COOH)_2(COO)_2\}^{2-}$ moieties, and further bonded to them through five sets of O–H···O hydrogen-bonding systems (Fig. S4) leading to the 3D supramolecular network of **1** (Fig. 2). Details of the hydrogen bonds are listed in Table S1.

As depicted in Fig. S5, the spectra of **L** and **1** are similar, both of them show strong absorption bands at high energy ($\lambda < 350$ nm) that can be assigned to the intraligand π–π* transition [24], and a moderate absorption band (350–600 nm) at lower energy can be assigned to intraligand charge-transfer (ILCT). The calculations at the density functional theory B3LYP/6-31G* level [25,26], available in Gaussian 03 [27], were carried out to understand the ILCT existed in ligand **L**.

As depicted in Fig. 3, in analogy to other donor-acceptor systems based on TTF [11], the HOMO distribution of ligand **L** primarily reside on the donor TTF skeleton, while the LUMO show large amplitudes on electron acceptor fragment – the carboxylic moiety. Therefore, the calculation determined value from the energy gap of the HOMO and the LUMO is 3.15 eV (486 nm), while the experimental determined value is 492 nm. Good agreement between calculation and experiment data